Dielectric relaxation and charged domain walls in (K,Na)NbO_3-based ferroelectric ceramics

A. A. Esin, D. O. Alikin, A. P. Turygin, A. S. Abramov, J. Hreščak, J. Walker, T. Rojac, A. Bencan, B. Malic, A. L. Kholkin, and V. Ya. Shur

Citation: J. Appl. Phys. **121**, 074101 (2017); doi: 10.1063/1.4975341
View online: http://dx.doi.org/10.1063/1.4975341
View Table of Contents: http://aip.scitation.org/toc/jap/121/7
Published by the American Institute of Physics

Dielectric relaxation and charged domain walls in (K,Na)NbO_3-based ferroelectric ceramics

A. A. Esin,[1] D. O. Alikin,[1] A. P. Turygin,[1] A. S. Abramov,[1] J. Hreščak,[2] J. Walker,[3] T. Rojac,[2] A. Bencan,[2] B. Malic,[2] A. L. Kholkin,[1,4] and V. Ya. Shur[1,a)]
[1]*Institute of Natural Sciences and Mathematics, Ural Federal University, Ekaterinburg, Russia*
[2]*Electronic Ceramics Department, Jožef Stefan Institute, 1000 Ljubljana 620006, Slovenia*
[3]*Materials Research Institute, Pennsylvania State University, University Park, Pennsylvania 16802, USA*
[4]*Physics Department and CICECO–Aveiro Institute of Materials, University of Aveiro, 3810-193, Aveiro, Portugal*

(Received 2 November 2016; accepted 17 January 2017; published online 15 February 2017)

The influence of domain walls on the macroscopic properties of ferroelectric materials is a well known phenomenon. Commonly, such "extrinsic" contributions to dielectric permittivity are discussed in terms of domain wall displacements under external electric field. In this work, we report on a possible contribution of charged domain walls to low frequency (10–10^6 Hz) dielectric permittivity in $K_{1-x}Na_xNbO_3$ ferroelectric ceramics. It is shown that the effective dielectric response increases with increasing domain wall density. The effect has been attributed to the Maxwell-Wagner-Sillars relaxation. The obtained results may open up possibilities for domain wall engineering in various ferroelectric materials. *Published by AIP Publishing*. [http://dx.doi.org/10.1063/1.4975341]

I. INTRODUCTION

The piezoelectric device market is dominated by lead containing $Pb(Zr_{1-x},Ti_x)O_3$ (PZT) based materials due to their versatility and robust functional properties. The toxicity of lead, however, has raised health and environmental concerns and in the last two decades, legislative changes have stimulated intensive research into suitable lead-free PZT alternative materials.[1] Among the numerous investigated lead-free oxides and solid solutions, $K_{1-x}Na_xNbO_3$ (KNN) based systems have received enormous attention after publications by Saito *et al*. in 2004, who reported piezoelectric coefficients for KNN comparable to PZT.[2,3]

Despite the significant focus on KNN-based ceramics and the subsequent wave of scientific publications, commercial realization of its piezoelectric properties has not been forthcoming due to the difficult processing of the material in the bulk ceramic form. The main problem of KNN ceramics synthesis is the difficulty in achieving high bulk density and reproducible electrical properties.[3–5] Various strategies have been used to overcome this problem.[4,6–8] It has been shown that the addition of 0.5 at. % of Sr^{2+} causes an increase in the relative density of the ceramics up to 96% and improves its functional response.[9] Moreover, KNN solid solution remains in orthorhombic perovskite phase at room temperature, while dielectric permittivity shows a great increase (above 3 times) in high degree (5%) doped KNN.[9,10] Doping with Sr^{2+} with concentration above 2% has a two-fold effect: in the frequency range from 10 to 1000 kHz dielectric permittivity increases, but the piezoelectric coefficient apparently decreases.[9,10]

A thorough analysis of the relationships between variation of grain sizes, domain wall density, and functional properties of ferroelectric ceramics requires careful consideration of the domain wall contribution, including their charge state and mobility. It is known that the dielectric properties can be influenced by domain walls in ferroelectric thin films,[11,12] ceramics,[13,14] and single crystals.[15,16] Reversible and irreversible displacements of domain walls in AC electric fields are considered as common mechanisms that contribute to dielectric and piezoelectric responses.[13–15,17] Recently, a contribution of domain wall displacements to dielectric permittivity has been also considered in KNN-based ceramics.[18,19] However, separation of the vibrational and stationary contributions of domain walls to dielectric permittivity is still under discussion.[20] As for another lead-free ceramic material, $BiFeO_3$, it was shown that the domain walls, due to their conductivity, could influence the macroscopic properties via linear and nonlinear Maxwell-Wagner mechanisms.[21] The influence of charged domain walls on the dielectric response was also considered in $BaTiO_3$ single crystals.[22]

In this contribution, we have studied in more detail the increase of the dielectric permittivity in KNN ceramics with Sr doping. While a number of different mechanisms may lead to such a behavior and may operate simultaneously in the material, we have found an apparent relationship between the density of charged domain walls, which are expected to exhibit enhanced conductivity, and the increase of the dielectric permittivity at low frequencies. The results thus suggest a possible role of charged domain walls in the dielectric dispersion through Maxwell-Wagner effects.

II. EXPERIMENTAL

The investigated samples of KNN ceramics doped by strontium ions with nominal chemical formulations $(K_{0.5}Na_{0.5})_{1-2x}Sr_xNbO_3$, x ranging from 0 to 0.15, were prepared by a conventional solid-state method. We used the short abbreviations of the samples: KNN, KNN-1% Sr, KNN-2% Sr, etc. The details of the samples' preparation, their crystal structure, and phase composition are reported elsewhere.[23]

a)vladimir.shur@urfu.ru

The samples were polished with a gradual decrease of diamond abrasive down to 0.25 μm and final mechano-chemical strain-free polishing with colloidal silica with the particle size below 100 nm.[24] Dielectric permittivity has been measured using an impedance bridge QuadTech RLC 7600 (IET Labs Inc. USA) with $U_{AC} = 1$ V RMS AC voltage excitation. Scanning electron microscopy (SEM) realized with an Auriga Crossbeam Workstation (Carl Zeiss, Germany) was used to inspect the sizes of ceramic grains. The SEM was done on fracture ceramics. The grain size was estimated from the SEM images through the measurements of the average area occupied by the grains and calculation of their Feret's diameter. The domain structure was studied using a Probe Nanolaboratory NTEGRA Aura (NT MDT, Russia) and a Scanning Probe Microscope MFP-3D (Asylum Research, USA) in piezoresponse force microscopy (PFM) mode realized with internal electronics. All measurements have been done on the surfaces cleaned with acetone at room temperature in an atmosphere of dry nitrogen (humidity less than 5%) provided by constant gas flow through the microscope chamber. More detailed description of experimental procedures is presented in the supplementary material section.

III. RESULTS AND DISCUSSION

A. Dielectric measurements

We have found that the results of dielectric measurements of KNN ceramics are drastically dependent on the relative humidity (RH). The results obtained at low (RH < 10%) and high (RH > 80%) humidity were essentially different, especially at low frequencies (below 10 kHz) and for the high level of Sr^{2+} doping (see supplementary material). Exposure of the samples in a vacuum chamber with pressure about 10^{-5} Torr for 24 h resulted in a significant decrease of the low frequency dielectric permittivity and tanδ. The subsequent exposure to a vacuum did not change the properties. This fact sheds light on the well known irreproducibility of the KNN dielectric and piezoelectric properties[4] because of the absence of humidity control during ceramics characterization. More detailed structural characterization is necessary for clear understanding of the phenomena. In the following, all dielectric and PFM measurements were performed with KNN samples dried under vacuum conditions.

Both low and high frequency dielectric permittivity demonstrated significant enhancement for KNN with 0%–2% Sr^{2+} doping level. For higher concentrations, they remain almost constant and even decrease for 8% and 15% (Fig. 1). This dependence is similar to that for the d_{33} piezoelectric coefficient in Sr^{2+} doped KNN revealed by Malic *et al.*[10] and cannot be attributed to porosity, as the ceramics density was similar irrespective of the Sr concentration (see the supplementary material). The microstructure and domain structure were inspected for deeper understanding of the KNN dielectric properties.

B. Morphology of the grains and domain structure

Undoped KNN ceramics consists of relatively large (1–5 μm) cubic-shaped grains (Fig. 2(a)). Doping of ceramics

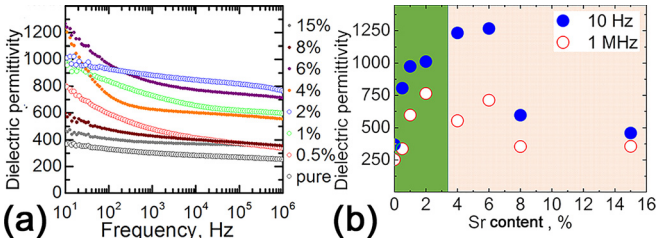

FIG. 1. Dielectric properties of the Sr^{2+} doped KNN ceramics. (a) Frequency dependence of dielectric permittivity KNN ceramics with different compositions (imaginary part is presented in supplementary material); (b) dependence of dielectric permittivity on Sr^{2+} content. Orange region marks the range of compositions with a "single grain–single domain region."

with Sr^{2+} in the range from 0.5% to 2% led to a decreasing fraction of large grains (Fig. 2(a)) and the appearance of both close to cubic and randomly shaped grains with sizes in the range 300 nm–1 μm. Doping of KNN ceramics above 4% Sr^{2+} resulted in significant grain size reduction. Randomly shaped grains became dominant in KNN with a doping level above 6%. The distribution of grain sizes became narrower and decreased gradually with increasing Sr^{2+} content (Figs. 2(b) and 2(c)).

Doping of ceramics resulted in a gradual decrease of the average domain size (along with the decrease of the grain size) down to values below the PFM resolution limit (Fig. 3). Analysis of the domain images revealed the following two types of the domain structures:

1. Conventional domain structure for non-polarized ceramics with herringbone, watermark, and zigzag shapes obtained in the ceramics with a low doping level (0–1% Sr^{2+}).[25]
2. "Single grain–single domain" structure has been obtained for the ceramics with the doping level above 6% Sr^{2+}. This structure studied by transmission electron microscopy (TEM) (see supplementary material) can be attributed to the grain size effect.[26]

The mixture of both types of the domain structures was revealed for ceramics with an intermediate doping level (2–4% Sr^{2+}). Moreover, the appearance of the regions without a piezoresponse and increase of their fraction with doping (orange color with average intensity in Fig. 3) were also observed. This can be attributed to the appearance of secondary phases, in agreement with structural characterization.[23] Appearance of the secondary phase obviously leads to a decrease in the dielectric permittivity of highly doped KNN ceramics (see Fig. 1(a)).

It is known that domain walls can influence the ferroelectric, dielectric, and piezoelectric properties in a number of ways;[13–15,17] an important aspect is their state of charge.[27,28] In fact, theory predicts that band bending at charged domain walls, for example, at tail-to-tail or head-to-head domain walls, results in increased electrical conductivity at the walls, which may exceed that of the bulk crystal by orders of magnitude.[27] For this reason, we looked in more detail into the charge state of domain walls in KNN with different Sr contents.

Vector PFM analysis[29] allows us to extract the projection of spontaneous polarization in plane and to reveal the relative

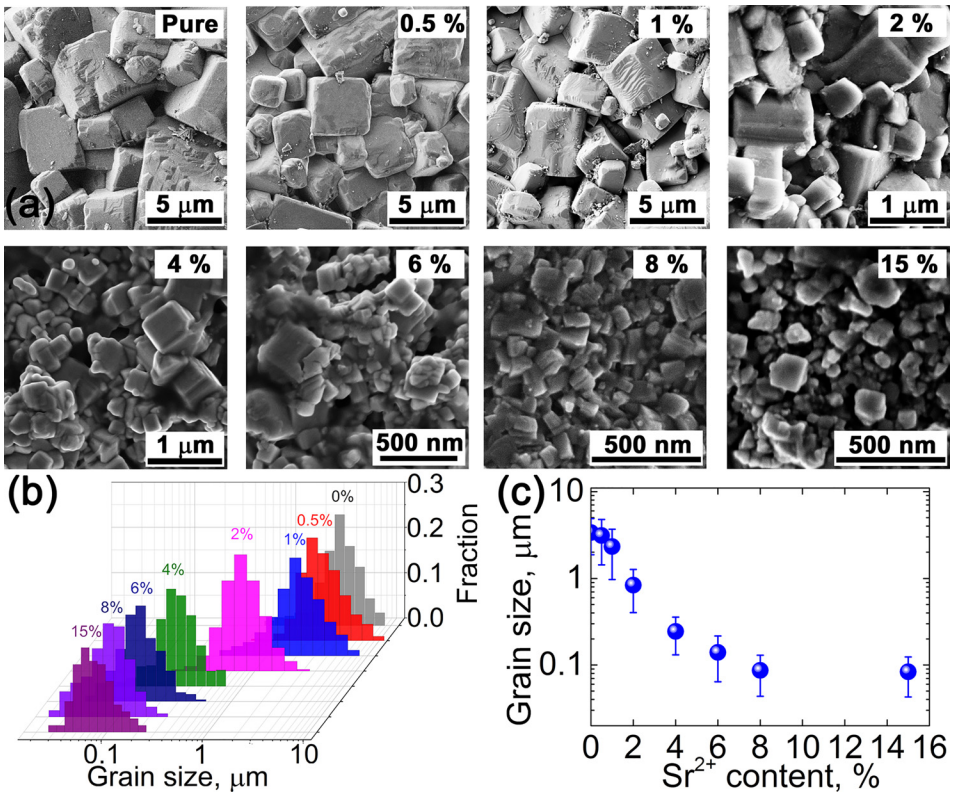

FIG. 2. (a) SEM images of the KNN fractured surface of ceramics with various Sr^{2+} contents. (b) Grain size distribution for various doping levels; (c) dependence of the average grain size on Sr^{2+} content. Dispersion of the grain size is indicated by error bars.

concentration of charged domain walls (Fig. 4). The measurement of the angle between spontaneous polarization vectors in neighboring domains separated by a given domain wall allowed us to discriminate the charged and neutral walls (Figs. 4(b) and 4(c)). The relative concentrations of 180° and non-180° domain walls and grain boundaries determined by the calculation of their total length are summarized in Table I. The concentration of nominally charged domain walls was between 30% and 40%. It is necessary to keep in mind that according to recent experimental research almost all 180° ferroelectric domain walls are deviated from the polar axis and therefore are charged.[30,31]

Analysis of vector PFM images used to determine the average density of domain walls was performed on ceramics with Sr^{2+} content below 2% with multidomain grains and large enough domains for PFM visualization (the algorithm of analysis is presented in the supplementary material). The volume fraction of all (charged and non-charged) domain walls was

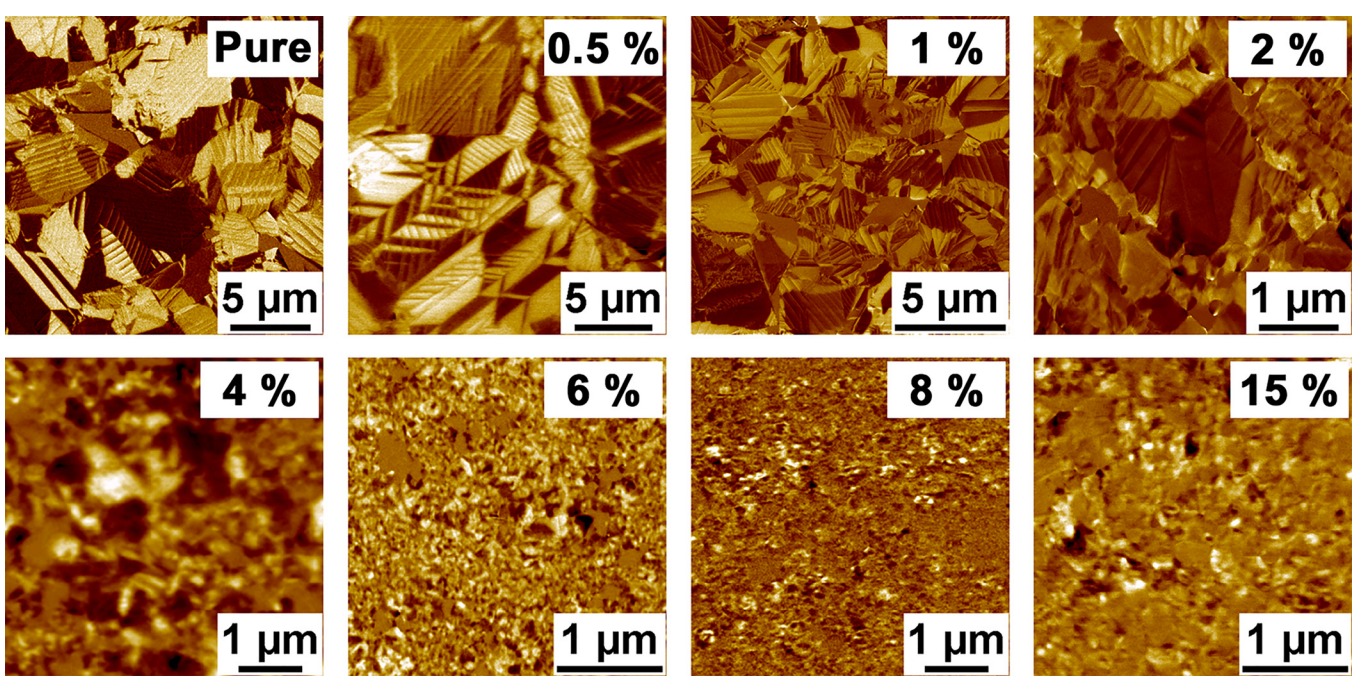

FIG. 3. PFM images of KNN ceramics with various Sr^{2+} contents obtained by mapping of the piezoresponse signal (R cos θ).

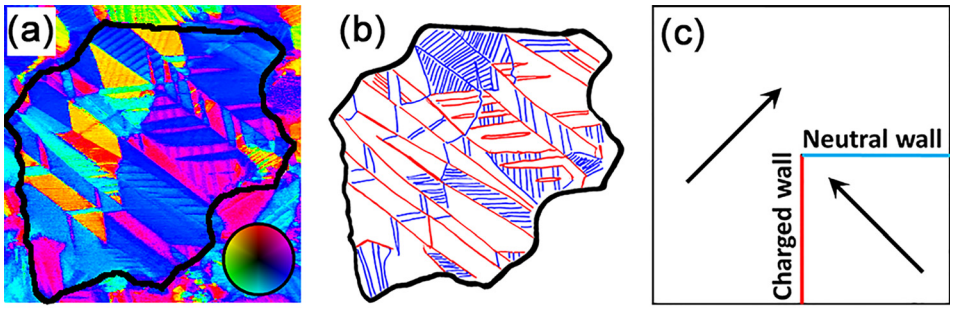

FIG. 4. (a) Image of the domain structure with vector representation of the PFM data. The grain boundary is marked in black. The orientation angle is color coded as shown with the "color wheel."[29] (b) Scheme of the domain walls in the grain. Charged and neutral domain walls are marked in red and blue, respectively. (c) Schematics demonstrating the difference in orientations of charged and neutral domain walls. The colors correspond to the "color wheel" in (a).

TABLE I. Relative concentrations of domain walls and grain boundaries for various Sr^{2+} contents.

Composition	Non-180° domain walls	180° domain walls	Grain boundaries
KNN	0.65	0.2	0.15
KNN 0.5% Sr	0.66	0.19	0.15
KNN 1% Sr	0.72	0.15	0.13
KNN 2% Sr	0.57	0.19	0.24

extracted by the analysis of PFM images assuming that the domain wall width equals to 1 nm and uniform domain wall density at the surface and in the bulk (Figs. 5(a) and 5(b)). The domain orientation is given in Figure 5(a), while the revealed charged and non-charged domain walls are shown in Figure 5(b). It was demonstrated that the dielectric permittivity of doped KNN ceramics increased with increasing domain wall volume (Fig. 5(c)).

C. Relation between dielectric behavior and microstructure

The smooth dispersion of the dielectric permittivity with a rise at low frequencies is illustrated in Fig. 1(a). Such behavior has already been observed in different systems and can be described from different points of view: displacements of domain walls under sub-coercive electric field loading,[13,14,18,19] Maxwell-Wagner relaxation caused by so-called electrical inhomogeneities, for example, due to differences between the values of the dielectric permittivity and dc conductivity of the grains and at the grain boundaries,[32,33] polaron hopping conductivity, or Schottky barriers near the electrode area.[34,35]

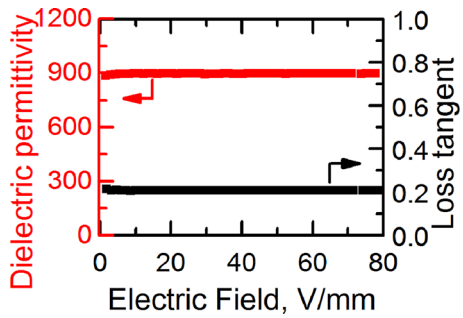

FIG. 6. Dielectric permittivity in KNN ceramics doped by 1% Sr^{2+} dependence on AC electric field amplitude at the frequency of 500 Hz.

We cannot rule out a possible influence of hopping conductivity on the dielectric permittivity, which is widely discussed in PZT ceramics.[36] However, another possibility to consider is the influence of charged domain walls on dielectric permittivity, which may arise due to displacements of domain walls under field or the presence of elevated conductivity at the walls or combination of both.[21] In the case of irreversible domain wall displacements, one expects a dependence of the dielectric permittivity on the amplitude of electric field.[37] In contrast, according to our measurements, the dielectric permittivity in KNN does not depend on the electric field amplitude up to 80 V/mm (Fig. 6); however, domain walls may still move reversibly, thus contributing to the linear part of the dielectric permittivity.

Considering the significant amount of charged non-180° and 180° domain walls in KNN ceramics (see Table I) and the dependence of dielectric permittivity on the domain wall density, we suggest their influence as conductive inclusions into a dielectric matrix. Supporting this is the experimentally confirmed fact that approximately half of the charged

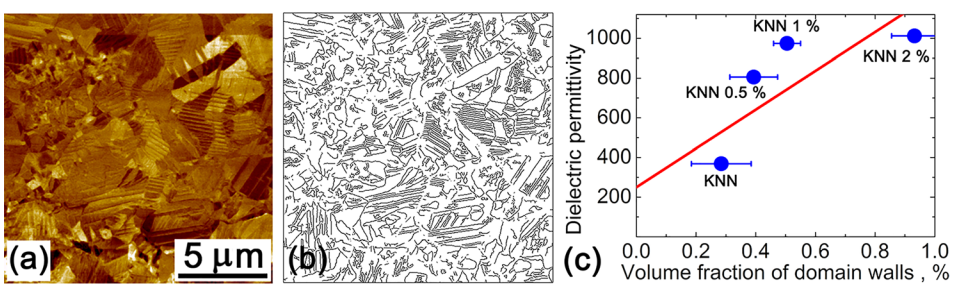

FIG. 5. (a) In-plane PFM image. (b) Domain walls extracted by analysis of the PFM image (grain boundaries are excluded) (see the supplementary material). (c) Experimental data (blue dots) and theoretical dependence (red line) of the dielectric permittivity at 10 Hz on the volume fraction of domain walls (charged and non-charged).

domain walls has essentially higher electrical conductivity than the bulk.[38] In light of the predicted enhanced electrical conductivity at domain walls,[38] it is thus possible that these conductive features create Maxwell-Wagner relaxation effects. While we cannot exclude contributions from alternative sources of electrical inhomogeneity, the possible role of grain boundaries is likely minor because their concentration is significantly smaller than that of charged domain walls in ceramics doped with Sr^{2+} in concentrations lower than 2% and does not vary significantly as a function of the Sr content (see Table I) despite the significant increase in the dielectric permittivity (see Fig. 1(a)).

We have performed theoretical calculations of dielectric permittivity for ceramics with charged domain walls according to the Maxwell-Wagner-Sillars model for the medium with dispersed conductive inclusions. Charged domain walls were considered as conductive ellipsoids with high aspect ratio n equal to the ratio between the average grain size and domain wall thickness. The value of dielectric permittivity of charged domain walls was taken as dielectric permittivity in the paraelectric phase of KNN.[10] Under these approximations, the expression from the Maxwell-Wagner-Sillars model[39] is reduced to Debye-type dispersion

$$\varepsilon_{eff} = \varepsilon_1 + \frac{q \cdot n \cdot \varepsilon_1}{(1+\omega^2\tau^2)}, \tag{1}$$

where ε_1 dielectric permittivity of the grain, $\tau = \varepsilon_1 \cdot n/4\pi\sigma_2$ is the relaxation time, σ_2 is the domain wall conductivity, and q is the volume fraction of the charged domain walls.

Integration of Eq. (1) for normal distribution of n confined by dispersion Δn determined by the average grain size gives the following equation for the effective dielectric permittivity:

$$\begin{aligned}\varepsilon_{eff} &= \varepsilon_1 + \int_0^\infty \frac{2}{\Delta n^2} n e^{-\left(\frac{n}{\Delta n}\right)^2} \frac{\varepsilon_1 n q}{1+\omega^2\tau^2} dn \\ &= \varepsilon_1 + \frac{2q}{\Delta n^2}\frac{\sqrt{\pi}}{2}\left(\frac{\varepsilon_1 \Delta n}{\omega^2\tau^2} - \frac{\varepsilon_1}{\omega^3\tau^3}\sqrt{\pi}\, e^{\frac{1}{\tau^2\omega^2\Delta n^2}} Erfc\left(\frac{1}{\tau\omega\Delta n}\right)\right),\end{aligned} \tag{2}$$

where $Erfc(x) = \frac{2}{\pi}\int_x^\infty e^{-t^2} dt$ is the Gauss error function.

The calculated dependencies of the dielectric permittivity on frequency for different values of domain wall conductivity are presented in Figure 7(a). Variation of conductivity change from $10^{-7}\,\mathrm{O\,m^{-1}\,cm^{-1}}$ (two orders higher bulk conductivity[40]) to $10^{3}\,\mathrm{O\,m^{-1}\,cm^{-1}}$ (metal conductivity) leads to τ shift from 10 to 10^{-6} s. Nevertheless, the integration of Eq. (2) by the time constant encounters difficulties with introduction of appropriate distribution of relaxation times. It must be noted that inhomogeneity of the ceramic system and random domain wall orientation lead to significant complication of the model in comparison with a simple Maxwell-Wagner-Sillars model. The appearance of such anomalous dielectric relaxation in disordered systems supports the Cole-Cole empirical expressions[41,42]

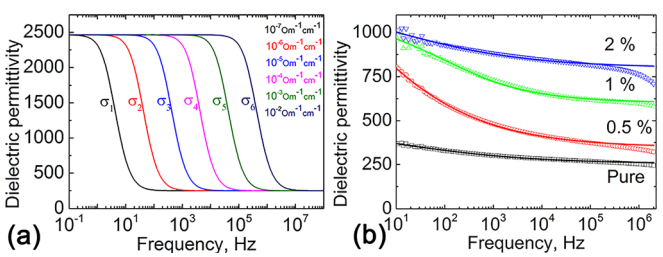

FIG. 7. Frequency dependences of dielectric permittivity: (a) calculated from Eq. (2) for different inclusion conductivities, (b) measured in KNN ceramics with different Sr^{2+} contents fitted by Eq. (3).

$$\varepsilon_{eff} = \varepsilon_1 + \frac{\Delta\varepsilon(1+(\omega\tau)^{1-\alpha}\sin(\pi\alpha/2))}{1+2(\omega\tau)^{1-\alpha}\sin(\pi\alpha/2)+(\omega\tau)^{2(1-\alpha)}}, \tag{3}$$

where α has a mathematical meaning of "broadening" parameter, and $\Delta\varepsilon$ is the Maxwell-Wagner assisted dielectric contribution.

Equation (3) is the mathematical expression of the idea that the dielectric permittivity represents a collection of individual components each being described by a Debye equation with its own relaxation time.[41] Fitting of the experimental data for KNN with Sr^{2+} content below 2% gives reasonable results. α is found to be in the range of 0.6 to 0.7 for all compositions, which is close to the typical value for the disordered systems (Figure 7(b)).[43,44] The wide range of τ from 10 ms to 1 s can be attributed to variations in the domain wall geometry and conductivity.

The theoretical curve with experimental parameters and domain wall conductivity of $2\times10^{-7}\,\mathrm{O\,m^{-1}\,cm^{-1}}$ plotted according to Eq. (2) is close to the obtained experimental data (Fig. 5(c)). The chosen conductivity value is only two orders of magnitude higher than the bulk conductivity;[40] however, the existence of a high density of domain walls with conductivity significantly lower than the metallic one may still result in strong variation of the dielectric permittivity. Thus, careful control of the domain structure is indispensable for the improvement of the dielectric and piezoelectric performance of ferroelectric ceramics.

IV. CONCLUSION

In conclusion, we proposed that an extrinsic mechanism possibly contributes to the dielectric permittivity of KNN ceramics at low frequencies. This mechanism is based on the experimentally observed existence of charged domain walls in KNN-based ceramics. We considered the charged domain wall as conductive inclusions, affecting the dielectric permittivity according to the Maxwell-Wagner-Sillars model for materials with inhomogeneous electrical conductivity. It was shown that the dielectric permittivity increases with increasing domain wall density. Frequency dependence of dielectric permittivity for KNN with different compositions has been fitted by the Cole-Cole equation and the estimated α parameter was found typical for disordered systems. The source of disorder in our case could be the continuous distribution of charged domain walls with different orientations in the volume of ceramics. Simple considerations in the frame of the Maxwell-Wagner-Sillars model indicate that the existence of sufficiently conductive domain walls with high density could

be the reason for the pronounced increase of the dielectric permittivity in KNN-based ceramics, although other mechanisms, such as polaron hopping conductivity, might also contribute to the dielectric permittivity.

SUPPLEMENTARY MATERIAL

See supplementary material for the experimental details of dielectric permittivity measurements, experimental details of microscopic measurements, humidity dependence of KNN dielectric properties, imaginary part of dielectric permittivity, and algorithm of domain structure analysis.

ACKNOWLEDGMENTS

The equipment of the Ural Center for Shared Use "Modern Nanotechnology" UrFU has been used. The research was made possible by the Ministry of Education and Science of Russian Federation (UID RFMEFI58715X0022). The authors acknowledge E. L. Rumyantsev and M. Morozov for useful discussion.

[1]J. Rödel, W. Jo, K. T. P. Seifert, E. M. Anton, T. Granzow, and D. Damjanovic, J. Am. Ceram. Soc. **92**, 1153 (2009).
[2]Y. Saito, H. Takao, T. Tani, T. Nonoyama, K. Takatori, T. Homma, T. Nagaya, and M. Nakamura, Nature **432**, 84 (2004).
[3]M. Kosec, B. Malič, A. Benčan, and T. Rojac, in *Piezoelectric and Acoustic Materials for Transducer Applications*, edited by A. Safari and E. K. Akdoğan (Springer, New York, 2008), pp. 81–103.
[4]B. Malič, J. Koruza, J. Hreščak, J. Bernard, K. Wang, J. Fisher, and A. Benčan, Materials **8**, 8117–8146 (2015).
[5]I. Coondoo, N. Panwar, and A. Kholkin, J. Adv. Dielectr. **3**, 1330002 (2013).
[6]R. E. Jaeger and L. Egerton, J. Am. Ceram. Soc. **45**, 209–213 (1962).
[7]M. Kosec and D. Kolar, Mat. Res. Bull. **10**, 335–340 (1975).
[8]Z. S. Ahn and W. A. Schulze, J. Am. Ceram. Soc. **70**, 18–21 (1987).
[9]B. Malic, J. Bernard, J. Holc, D. Jenko, and M. Kosec, J. Eur. Ceram. Soc. **25**, 2707–2711 (2005).
[10]B. Malic, J. Bernard, J. Holc, and M. Kosec, Ferroelectrics **314**, 149–156 (2005).
[11]D. V. Taylor and D. Damjanovic, Appl. Phys. Lett. **73**, 2045–2047 (1998).
[12]D. V. Taylor and D. Damjanovic, J. Appl. Phys. **82**, 1973–1975 (1997).
[13]N. A. Pertsev and G. Arlt, Ferroelectrics **132**, 27–40 (1992).
[14]N. A. Pertsev and G. Arlt, J. Appl. Phys. **74**, 4105–4112 (1993).
[15]A. Glazounov and A. K. Tagantsev, Ferroelectrics **221**, 57–66 (1999).
[16]V. Ya. Shur, E. L. Rumyantsev, E. V. Nikolaeva, and E. I. Shishkin, Appl. Phys. Lett. **77**, 3636–3638 (2000).
[17]E. Buixaderas, V. Bovtun, M. Kempa, M. Savinov, D. Nuzhnyy, F. Kadlec, P. Vanek, J. Petzelt, M. Eriksson, and Z. Shen, J. Appl. Phys. **107**, 014111 (2010).
[18]J. Zhang, W. Hao, Y. Gao, Y. Qin, Y. Tan, and C. Wang, Appl. Phys. Lett. **101**, 252905 (2012).
[19]Y. Huan, X. Wang, L. Li, and J. Koruza, Appl. Phys. Lett. **107**, 202903 (2015).
[20]R. Xu, J. Karthik, A. R. Damodaran, and L. W. Martin, Nat. Commun. **5**, 3120–3127 (2014).
[21]T. Rojac, H. Ursic, A. Bencan, B. Malic, and D. Damjanovic, Adv. Funct. Mater. **25**, 2099–2108 (2015).
[22]T. Sluka, A. K. Tagantsev, D. Damjanovic, M. Gureev, and N. Setter, Nat. Commun. **3**, 748–755 (2012).
[23]J. Hreščak, A. Bencan, T. Rojac, and B. Malič, J. Eur. Ceram. Soc. **33**, 3065–3075 (2013).
[24]T. Doi, E. Uhlmann, and I. Marinescu, *Handbook of Ceramics Grinding and Polishing* (Elsevier, 2015).
[25]Y. Qin, J. Zhang, W. Yao, C. Wang, and S. Zhang, J. Am. Ceram. Soc. **98**, 1027–1033 (2015).
[26]C. Fang, L. Chen, and D. Zhou, Phys. B: Condens. Matter **409**, 83–86 (2013).
[27]E. A. Eliseev, A. N. Morozovska, G. S. Svechnikov, V. Gopalan, and V. Y. Shur, Phys. Rev. B **83**, 235313 (2011).
[28]T. Sluka, A. K. Tagantsev, P. Bednyakov, and N. Setter, Nat. Commun. **4**, 1808 (2013).
[29]S. V. Kalinin, B. J. Rodriguez, S. Jesse, J. Shin, A. P. Baddorf, P. Gupta, H. Jain, D. B. Williams, and A. Gruverman, Microsc. Microanal. **12**, 206–220 (2006).
[30]M. Schröder, A. Haußmann, A. Thiessen, E. Soergel, T. Woike, and L. M. Eng, Adv. Funct. Mater. **22**, 3936–3944 (2012).
[31]D. Meier, J. Seidel, A. Cano, K. Delaney, Y. Kumagai, M. Mostovoy, N. A. Spaldin, R. Ramesh, and M. Fiebig, Nat. Mater. **11**, 284–288 (2012).
[32]H. Neumann and G. Arlt, Ferroelectrics **69**, 179–186 (1986).
[33]D. Damjanovic, M. Demartin Maeder, P. Duran Martin, C. Voisard, and N. Setter, J. Appl. Phys. **90**, 5708–5712 (2001).
[34]X. Martí, P. Ferrer, J. Herrero-Albillos, J. Narvaez, V. Holy, N. Barrett, M. Alexe, and G. Catalan, Phys. Rev. Lett. **106**, 236101 (2011).
[35]M. I. Morozov, M. A. Einarsrud, and T. Grande, J. Appl. Phys. **115**, 044104 (2014).
[36]M. I. Morozov and D. Damjanovic, J. Appl. Phys. **107**, 034106 (2010).
[37]G. Arlt and N. A. Pertsev, J. Appl. Phys. **70**, 2283–2289 (1991).
[38]T. Sluka, A. K. Tagantsev, P. Bednyakov, and N. Setter, Nat. Commun. **4**, 1808–1814 (2013).
[39]R. W. Sillars, J. Inst. Electr. Eng. **80**, 378–394 (1937).
[40]M. A. Rafiq, M. E. Costa, A. Tkach, and P. M. Vilarinho, Cryst. Growth Des. **15**, 1289–1294 (2015).
[41]B. K. P. Scaife, *Principles of Dielectrics* (Clarendon Press, Oxford, 1998).
[42]M. Schröder, X. Chen, A. Haußmann, A. Thiessen, J. Poppe, D. A. Bonnell, and L. M. Eng, Mater. Res. Express **1**, 035012 (2014).
[43]P. A. M. Steeman and F. H. J. Maurer, Colloids Polym. Sci. **270**, 1069–1079 (1992).
[44]O. Petracic, S. Sahoo, C. Binek, W. Kleemann, J. B. Sousa, S. Cardoso, and P. P. Freitas, Phase Trans. **76**, 367–375 (2003).